Magnetic Properties of Enriched 195Pt Metals

doi: 10.1007/s10909-009-9865-3

Magnetic Properties of Enriched ^{195}Pt Metals

N. Kuwata, K. Ohno, E. Kobayashi, Y. Sugita, and H. Suzuki
Department of Physics, Faculty of Science, Kanazawa University
Kakuma-machi, Kanazawa 920-1192, Japan

An enriched ^{195}Pt system was investigated by magnetic and NMR measurements. Anomalous large magnetic moments are distinctly observed in enriched ^{195}Pt wire samples produced by ORNL and in enriched thin-film samples. In the enriched powder and natural wire samples, weak anomalous large magnetic moments were also observed in magnetic measurements. These anomalous large magnetic moments were discussed by the induced giant magnetic moments of Fe impurity. The induced magnetic moments are different in wire samples and powder samples.

1. INTRODUCTION

The nuclear magnetic orderings of pure metals have been observed in Cu [1], Ag [2] and Sc [3]. All these nuclear magnetic orderings have been achieved by two-stage nuclear demagnetization cooling, namely, the first nuclear stage made of massive copper and the second nuclear stage, a sample metal, without a thermal heat switch between the first and second nuclear stages. Nuclear spins were only cooled down below the nuclear magnetic ordering temperatures $T_{C,n}$ = 60 nK, 560 pK and 2 μK for Cu, Ag and Sc, respectively. During these experiments, conduction electrons stayed at much higher temperatures than nuclei. These conditions can exist in metals at very low temperatures, which have a weak

coupling between electrons and nuclei expressed by the Korringa constant κ with $\kappa \geq 1$ Ks as Cu (κ = 1.2 Ks), Ag (κ = 12 Ks) [4] and Sc (κ = 1.6 Ks) [5]. To achieve nuclear magnetic ordering in thermal equilibrium, we have to choose metals that have short spin-lattice relaxation times and to use a heat switch between the first and second nuclear stages of the sample metal. One candidate metal is platinum with κ = 0.3 Ks. Among isotopes of Pt, only ^{195}Pt has the nuclear spin I = 1/2 with the nuclear magnetic moment μ = 0.597 μ_N. The natural abundance of ^{195}Pt is 33.8 %. For the natural isotopic mixture of Pt, the nuclear magnetic ordering temperature is expected to be lower owing to the small number of nearest neighbors. However, using an enriched ^{195}Pt nuclear spin system, we can change the concentration of the nuclear spin without changing the electronic state. This should be an ideal system for investigating the concentration dependence of magnetism.

We started to investigate an enriched ^{195}Pt system. Before starting the nuclear demagnetization experiment, we measured the magnetic susceptibility of an enriched ^{195}Pt specimen using a SQUID magnetometer. Interesting but rather unexpected results were obtained, which could be due to the characteristic property of the Pt metal. We

reported the results and gave plausible explanations in this paper.

2. SAMPLES

An isotopically 97.3 and 80%-enriched ^{195}Pt wire specimens of 0.5 mm diameter were prepared by the Oak Ridge National Laboratory (ORNL). According to the report by ORNL, an isotopically enriched wire is prepared as follows: 1) Enriched powders are pressed into a cylindrical shape. 2) The pressed cylindrical powders are arc-melted into an ingot. 3) The ingot is rolled until it is shaped into a 0.127-cm-diameter rod. 4) Then the ingot is swaged into an approximately 0.048 cm diameter wire. An "enriched 33.8%" wire which had natural concentration of isotopes was also prepared in the same way for comparison. We also used a 97.3 %-enriched ^{195}Pt film and powder specimens. As for the film specimen ORNL provided no report on the process. All these enriched specimens were prepared by ORNL. A natural Pt wire of 0.5 mm diameter and a natural powder specimen that were commercially available were also measured. Average sizes of powder specimens are approximately 40 μm. For some of these specimens, mass spectroscopic analysis of Fe impurity was performed at Toray Research Center, Inc.. As we have only a small amount 97% film sample and 80% sample, we did not performed the mass

spectroscopic analysis for them. The results are shown in Table 1. The enriched specimens contain more Fe impurities than the natural specimens. In the enriched wire specimens the amount of Fe impurity is roughly proportional to the ^{195}Pt content.

3. DC and AC MAGNETIC SUSCEPTIBILITY MEASUREMENTS

Dc magnetization and dc magnetic susceptibility, M/H, were measured using a SQUID magnetometer MPS system produced by Quantum Design Co., Ltd. between 1.8 and 300 K. Ac magnetic susceptibility was measured using a mutual impedance bridge (LR700 produced by Linear Research Co., Ltd.) in the low-temperature region produced by a nuclear demagnetized cryostat. The frequency used for LR700 mutual impedance bridge was 15.8 Hz.

4. EXPERIMENTAL RESULTS and DISCUSSION

The magnetization measured using a SQUID magnetometer in a field of 500 gauss are shown in Fig. 1 for several specimens. For easy comparison of the data, they are normalized to 100 at 300 K, as shown in Fig. 2. In the figures, the data of the 33.8 %-enriched wire represent the results for the 33.8 % (natural abundance) wire specimen produced by ORNL by the same process used for the 97.3 % wire. The

enriched wire samples including the 33.8 % wire sample show much larger magnetic susceptibilities than the other samples. As shown in Fig. 3, the normalized magnetic susceptibilities are expressed by Curie's law given as

$$X - X_0 = C/T, \text{ here Curie constant } C = Ng^2J(J+1)\mu_B^2/3k_B \equiv Np_{eff}^2\mu_B^2/3k_B. \quad (1)$$

Here X_0 is the extrapolated value at the high temperature limit.

From Curie's constant, the effective magnetic moment p_{eff} per ^{195}Pt atom was obtained to be 0.147, 0.142 and 0.141 μ_B for the 99.7 %, 80 % and 33.8 % specimens, respectively. The effective magnetic moments per ^{195}Pt atom are nearly the same for these specimens. Compared with the nuclear magnetic moment of ^{195}Pt, that is, 0.5965 μ_N, these effective magnetic moments are about 400 times as large as the pure nuclear magnetic moment. An 97.3 %-enriched thin film sample shows a weaker temperature dependence of magnetic susceptibility than the 97.3 % wire sample, but a much stronger than the powder and natural wire samples. On the other hand, the 97.3 %-enriched ^{195}Pt powder, natural powder and natural wire samples show an almost temperature-independent magnetic susceptibility in Fig. 2. However, in the expanded scale they also show the weak temperature dependence, as shown in Fig. 4. Among the three samples, the natural wire

sample shows the strongest temperature dependence of magnetic susceptibility. By fitting the magnetic susceptibilities of all the samples to Curie's law, the effective magnetic moments are determined and are listed in Table 2.

In Fig. 5, the ac magnetic susceptibilities below 1 K of the 97.3 % and 33.8 %-enriched wire specimens are shown. In the figure, the ac magnetic susceptibility is normalized to fit with the dc magnetic susceptibility at higher temperatures. The ac magnetic susceptibility shows a maximum at about 60 mK for the 97.3 % wire specimen and at about 20 mK for the 33.8 % one. For the 97.3 % specimen a magnetic field of 88 Oe was applied. The resultant magnetic susceptibility is also shown in the figure, represented by a solid line. Fig. 6 shows the magnetic field dependence of the magnetization of the wire samples at 2 K. It shows a tendency to saturate. At 50 K, the magnetization increases linearly with increasing magnetic field. The magnetization consists of two parts: a linear-magnetic-field-dependent magnetization expected of Pauli paramagnetism and an anomalous nonlinear-field-dependent part. In the inset of Fig. 7, the magnetizations of the 97.3 % film specimen at 2 K and 50 K are plotted against magnetic field. By subtracting the Pauli paramagnetic magnetization from the magnetizations of one at 2 K,

the resultant magnetization is shown in Fig. 7. Here the Pauli paramagnetic magnetization was obtained from the slope of *M-H* curve in the highest magnetic field limit. From the saturated magnetization, the effective magnetic moment per Pt atom is deduced to be 1.35 $\times 10^{-3}$ μ_B. Here, we used the relation

$$M = NgJ\mu_B \equiv Np'_{eff}\mu_B . \qquad (2)$$

Similarly the effective magnetic moments are obtained for all the other samples from the field dependence of magnetization, as shown in Table 3. When we deduced the effective magnetic moments per ^{195}Pt atom for the enriched wire samples, they are 2.17, 2.13 and 2.18 $\times 10^{-3}$ μ_B, which are approximately the same. In this case, the enhancement factor of the nuclear magnetic moment 1+K = 6.65 can be obtained. Here we describe the effective nuclear magnetic moment as $\mu_{Neff} = \gamma_{eff}\hbar I$, and the enhancement factor 1 + K = γ_{eff}/γ. Although the deviation from the linear dependence is rather small, the powder and natural wire samples also show a tendency to saturate with magnetic field, as shown in Fig. 8. The estimated effective magnetic moments, though it is so hard to estimate the values, are also listed in Table 3.

Now we will discuss the origin of the anomalous large magnetic moment observed in the

enriched ^{195}Pt specimen, particularly in the wire samples. The most possible origin of the anomalous magnetic moment should be due to the magnetic impurity, including defect or gas impurity. We tried to fit the field dependence of the magnetization to the Brillouin function of several J values, as shown in Fig. 9.

$$\mu_{JZ} = g_J \mu_B J B_J(y)$$

$$B_J(y) = \{(2J+1)/2J\} \coth\{(2J+1)y/2J\} - (1/2J) \coth\{y/2J\} \qquad (3)$$

Here, $y = Jg_J\mu_B H/k_B T$. In the figure, saturated values are normalized to one. The experimental results of the 97.3% film, 80% wire and 33.8 % wire show a good accordance; the 97.3% wire sample shows a slightly different field dependence. In the figure, the calculated magnetization curves for J = 1/2, 5/2, 4 and 10 are shown. If the ^{195}Pt nuclear magnetic moment contributes to the anomalous large magnetic moment, the calculated curve for J = 1/2 should be the best fit curve. However, the result is far from the accordance. If Fe^{3+} impurity is relevant to the anomalous large magnetic moment, the calculated curve for J = 5/2 should be the best fit curve. The fitting curve is rather close to the experimental data, but the best fit for the data of the 97.3% film, 80% wire and 33.8 % wire is the curve for J = 4, followed by a moderate move to larger values of J for larger

magnetic fields. And for the 97.3 % wire sample it is slightly deviated, but still the best fit is the curve for $J = 4$. Therefore, we cannot attribute the observed large magnetic moment to special localized magnetic impurity. It is well known that Fe impurities in Pt metal produce giant magnetic moments. Our experimental results can be also explained by the induced magnetic moment surrounding the Fe spins. The J values of the induced magnetic moments have a larger values of J than the Fe spin and distributed among the isolated Fe spins, as discussed by Herrmannsdörfer et al. [6]. They, however, obtained the best fitting curve of $J = \infty$ for their measured magnetic moment as a function of inverse temperature in the magnetic field.

Then when we attributed the anomalous magnetic moments to Fe impurities, the magnetic moments per Fe impurity were reduced and listed in Table 4 and 5. In these tables, it is found that the effective magnetic moments in powder samples are much smaller than those in wire samples. To author's knowledge, the magnetic properties have not yet been measured in powder $\underline{\text{Pt}}\text{Fe}_x$ samples. One plausible explanation for these smaller effective magnetic moments in powder samples can be the surface effect, because the powder samples have larger surface than the wire samples. The effective magnetic

moments determined from the magnetic susceptibility in Table 4 and those determined from the magnetization measurements in Table 5 are different to each others. For example, the effective magnetic moment $P_{eff} = 7.08 \pm 0.05\ \mu_B$ and $P_{eff} = 5.04 \pm 0.05\ \mu_B$ for 97.3 % wire in Table 4 and 5, respectively. The discrepancy is much more than the experimental error. If the effective number of the impurities is different from the amount of mass spectroscopic analysis data, we can explain it. It is because the number N and the effective magnetic moment P_{eff} appear in the different way in equations (1) and (2), that is, NP_{eff}^2 in eq. (1) and NP_{eff} in eq. (2). The self-consistent amounts of impurity are obtained to be 262 ppm for 97.3% wire samples and 102 ppm for 33.8% wire samples. In this estimation we used J=4 in equations (1) and (2). These amounts of impurities give rise to the value of effective magnetic moments as 8.0 and 7.3 μ_B, respectively. In the powder samples, the effective magnetic moment obtained from the magnetization measurements contains large error. So we will not discuss the discrepancy between the values in Table 4 and 5. Compared these smaller numbers of magnetic impurities N_{mag} with the mass spectroscopic analysis data N_{mass} it is found that the ratio N_{mag}/N_{mass} is almost constant, that is, 0.624 for 97.3% wire sample and 0.637 for 33.8% wire sample. Herrmannsdörfer

et al. also obtained the values of the giant magnetic moments in $\underline{Pt}Fe_x$ ($2.2 \leq x \leq 95$ ppm) from the temperature dependence of magnetization. Their samples were cut from the rods of 1 to 5 mm diameter. They found a weak increase of the effective magneton number with increasing impurity concentration x, starting from $P_{eff} = 7.6$ to $P_{eff} = 8.6\ \mu_B$. These values are nearly same value as our obtained value of 8 μ_B and 7.3 μ_B.

The electronic and nuclear magnetisms in $\underline{Pt}Fe_x$ at low temperatures have been discussed by Wendler et al. [7]. They observed the maximum magnetic susceptibility at 2.7 and 8.5 mK for x=11 and 41 ppm Fe in Pt samples. They attributed the maximum magnetic susceptibility to the occurrence of spin glass freezing. When we assume the linear dependence of maximum temperature on Fe concentration measured by Wendler et al. and apply the linearity to our experimental results, 60 mK for the 97.3 % wire sample shown in Fig. 6 gives rise to a 300 ppm concentration. Similarly, 20 mK for the 33.8 % wire sample corresponds to 100 ppm. These values are nearly same values which we obtained from the magnetic susceptibility and magnetization measurements. Pulsed NMR measurements have been performed on the 97.3 %-enriched ^{195}Pt wire, 33.8%-enriched wire, natural wire, 97.3%-enriched powder and natural powder samples

in the frequency range between 2 MHz and 30 MHz at 1.5 and 4.2 K. The measured Knight shift was K = -4.2 %, nearly the same as the previously reported values for all the specimens. The measured Korringa constant was T_1T = 30 msec K, which is in excellent agreement with the reported values in the measured frequency range. In our experiments, however, we did not measure the spin-lattice relaxation at low magnetic fields below 0.2 T. Therefore, no impurity effect on spin-lattice relaxation time can be observed. The decay of the spin-echo envelope shows two steps in the enriched wire samples. In Fig. 10, one of the typical results of the 33.8%-enriched wire sample is shown. The longer decay rate is nearly the same as that of the natural wire, which is also shown in the figure. Therefore, the short decay should be the decay of the nuclear spin influenced by the magnetic field of Fe giant magnetic moments, and the long one, the decay of the nuclear spin in bulk. In Fig. 11, the frequency dependence of T_2 is shown for the enriched ^{195}Pt wire, natural wire, 97.3 %-enriched powder and natural powder samples. In the figure, the short T_2 values are shown for 97.3% wire and 33.8% wire samples. It is reasonable to assume that the measured spin-spin relaxation time T_2* has two components, the intrinsic T_2 and T_{2in} due to the inhomogeneous magnetic field.

$1/T_2^* = 1/T_2 + 1/T_{2in}$

Since the inhomogeneous magnetic field ΔH which contains the inhomogeneity of the magnet and also the local inhomogeneous magnetic field due to the magnetic impurity moments, can be proportional to the applied magnetic field, that is, $\Delta H/H = \alpha_{mag.} + \chi_{loc.imp.}$, the following relation can be obtained,

$1/T_{2in} = 2\pi \cdot \gamma_n/2\pi \cdot \Delta H = 2\pi f \cdot \Delta H$. Here f is the frequency. As is evident from the figure, the measured T_2^* for 97.3% wire sample has the largest slope, corresponding to the largest $\chi_{loc.imp.}$ for this sample which is consistent with the magnetic measurement results. Summarizing our experimental result, all of anomalous behaviors can be understood by the magnetic impurities, mostly Fe impurity. Some of the results, however, are not consistent with each other.

1, The effective magnetic moments in powder samples are much smaller than those in wire samples.

2, The number of magnetic impurities N_{mag} obtained from the magnetic measurements is much smaller than the mass spectroscopic analysis data N_{mass}. It is found that the ratio N_{mag}/N_{mass} is almost constant, that is, 0.624 for 97.3% wire sample and 0.637 for 33.8%

wire sample.

To explain these discrepancies, the plausible explanation can be as follows,

1, Surface effect. The spatial distribution of electrons near the metal surface was investigated in small particles by Yu and Halperin [8]. They discussed Friedel oscillations of electron densities near the particle surface due to the boundary condition. If the Fe atoms near the surface produce the oscillating spin density, the effective magnetic moments can be reduced to some extent due to the cancellation.

2, Inhomogeneous distribution, such as clustering and segregation and so on.

By these effects we can explain our experimental results to some extent. But still there is a possibility of another explanation for our experimental discrepancy which we have not known yet.

CONCLUSION

The enriched ^{195}Pt system was investigated by magnetic and NMR measurements. Anomalous large magnetic moments are distinctly observed in the enriched ^{195}Pt wire samples produced by ORNL and in enriched thin-film sample. In the enriched powder and natural wire samples, small anomalous large magnetic moments were also observed

in magnetic measurements. These anomalous large magnetic moments can be explained by the giant magnetic moment produced by Fe impurities. The effective magnetic moments, however, in powder samples are much smaller than those in wire samples. And the number of magnetic impurities obtained from the magnetic measurements is much smaller than the mass spectroscopic analysis data. At present these still remain to be unknown. For our nuclear magnetism study with changing the ^{195}Pt nuclear spin concentration, it is better to use the powder specimens which contain less magnetic impurities. When we need the bulk specimen, we have to make by ourselves, preventing from the contamination.

REFERENCES

1. M. T. Huiku, T. A. Jyrkiö, J. M. Kyynäräinen, M. T. Loponen, O. V. Lounasmaa, and A. S. Oja, J. Low Temp. Phys. **62**, 433 (1986).
2. A. S. Oja, A. J. Annila, and Y. Takano, J. Low Temp. Phys. **85**, 1 (1991).
3. Y. Koike, H. Suzuki, S. Abe, Y. Karaki, M. Kubotaand H. Ishimoto, J. Low Temp. Phys. **101**, 617 (1995) ; H. Suzuki, Y. Koike, K. Karaki, M. Kubota and H. Ishinoto, Proc. of LT 21, 1996 Prague part **S4** 2183.
4. G. C. Carter and L. H. Bennet, Metallic Shifts in NMR, Pergamon Press, Oxford, 1st ed. (1977).
5. G. C. Carter, L. H. Bennet, and D. J. Kahan, Progress in Materials Science **20**, 295 (1977).
6. T. Herrmannsdörfer, S. Rehmann, W. Wendler, and F. Pobell, J. Low Temp. Phys. **104**, 49 (1996).

7. W. Wendler, T. Herrmannsdörfer, S. Rehmann, and F. Pobell, J. Low Temp. Phys. **111**, 99 (1998).
8. I. Yu and W. P. Halperin, J. Low Temp. Phys. **45**, 189 (1981).

TABLE 1

Concentrations of Fe impurity (ppm) determined by mass spectroscopic analysis.

97.3% wire	33.8% wire	natural wire	97% powder	natural powder
420 ± 5	160 ± 2	9.4 ± 0.05	180 ± 2	26 ± 0.2

TABLE 2

Effective magnetic moments obtained from Curie's constant for different-concentration samples of ^{195}Pt of different shapes. The unit of magnetic moment is μ_B.

sample / concentration	Wire	film	powder
97.3%	0.145 ± 0.001	0.125 ± 0.002	0.03 ± 0.001
80%	0.127 ± 0.002		0.022*±0.001
33.8%	0.082 ± 0.001		
Natural (33.8%)	0.023 ± 0.0005		0.015 ±0.0005

*: 86.6%

TABLE 3

Effective magnetic moment obtained from the saturated magnetization in 10^{-3} μ_B units.

Shape / Concentration	Wire	Film	Powder
97.3%	2.11 ±0.02	1.35· ± 0.015	0.076 ·
80%	1.7 ± 0.02		0.096*
33.8%	0.74		
Natural (33.8%)	0.063		0.065

*: 86.6%

TABLE 4

Effective magnetic moments per Fe impurity obtained from Curie's constant for different-concentration samples of ^{195}Pt of different shapes. The unit of magnetic moment is μ_B.

97.3% wire	80% wire	33.8% wire	natural wire	97.3% powder	natural powder
7.08 ± 0.05	6.7 ± 0.07	6.5 ± 0.03	7.5 ± 0.05	2.32 ± 0.06	4.3 ± 0.08

TABLE 5

Effective magnetic moment per Fe impurity obtained from the saturated magnetization in 10^{-3} μ_B units.

97.3% wire	80% wire	33.8% wire	natural wire	97.3% powder	natural powder
5.04 ± 0.05	4.72 ± 0.05	4.66 ± 0.05	6.7	0.43	2.0

FIGURE CAPTIONS

Fig. 1. Temperature dependence of magnetization measured at a magnetic field of 1 500 gauss. Denoted marks are as follows: 97.3%- enriched wire, red large open circle; 80%-enriched wire, blue closed circle; 33.8%-enriched wire, green small open circle; natural wire, orange x mark; 97.3%-enriched powder, red upward-triangle; 86.6%-enriched powder, blue downward-triangle; natural powder, orange cross; 97.3%-enriched film, red open square. (Color on-line)

Fig. 2. Temperature dependence of magnetic susceptibility (*M/H*) normalized to 100 at 300 K. Symbols are the same as those used in Fig.1. (Color on-line)

Fig. 3. Magnetic susceptibilities of Pt wire samples versus inverse temperature. Pauli paramagnetic components are subtracted from the measured magnetic susceptibilities. Symbols are the same as those used in the other figures. (Color on-line)

Fig. 4. Magnetic susceptibilities of enriched 97.3% powder (red upward-triangle), natural powder (orange cross) and natural wire (orange x mark) versus temperature in expanded scale. (Color on-line)

Fig. 5. AC magnetic susceptibilities below 1 K for 97.3%-enriched wire (red large open circle) and 33.8%-enriched wire (green small open circle). DC magnetic susceptibilities at higher temperatures are also shown. The ac magnetic susceptibility at a magnetic field of 88 Oe is also shown for the 97.3%-enriched wire by red solid line. (Color on-line)

Fig. 6. Magnetizations of wire samples measured at 2 K versus magnetic field. Symbols are the same as those in the other figures. (Color on-line)

Fig. 7. Saturation of magnetization of 97.3 %-enriched thin-film sample with magnetic field. Pauli paramagnetic component, that is, linear field dependent magnetization measured at 50 K (red closed squares in inset) is subtracted from the magnetization measured at 2 K (red open squares in inset). In the inset of the figure, the magnetizations measured at 50 K and at 2 K are shown. From the saturated value, an effective magnetic moment of $1.35 \cdot 10^{-3}$ μ_B was obtained. (Color on-line)

Fig. 8. Magnetizations of 97.3 % enriched powder at 2 K (red upward-triangle) and 50 K (closed triangle) versus magnetic field. (Color on-line)

Fig.9. Magnetizations of enriched samples, 97.3 % wire, 80 % wire, 33.7 % wire20and 97.3 % film measured at 2 K versus magnetic field. Calculated Brillouin functions for $J = 1/2$, 1, and 3/2 are shown by solid lines. All experimental results except those for the 97.3 % wire sample show a very good agreement and can be fitted well with the $J = 1$ curve. Experimental data for the 97.3 % wire fit rather well with the $J = 3/2$ curve. . Symbols are the same as those used in Fig.1. (Color on-line)

Fig. 10. Decay of NMR signal intensity. 33.8 %-enriched wire sample shows a two-step decay of the NMR signal. The longer decay time is nearly the same as the decay time of the natural wire . (Color 0n-line)

Fig. 11.Frequency dependence of spin-spin relaxation time T_2 measured at 4.2 K. In enriched wire samples only shorter T_2 values are shown. Natural wire and enriched powder sample show nearly the same T_2 values. Symbols are the same as those in the other figures. (Color on-line)

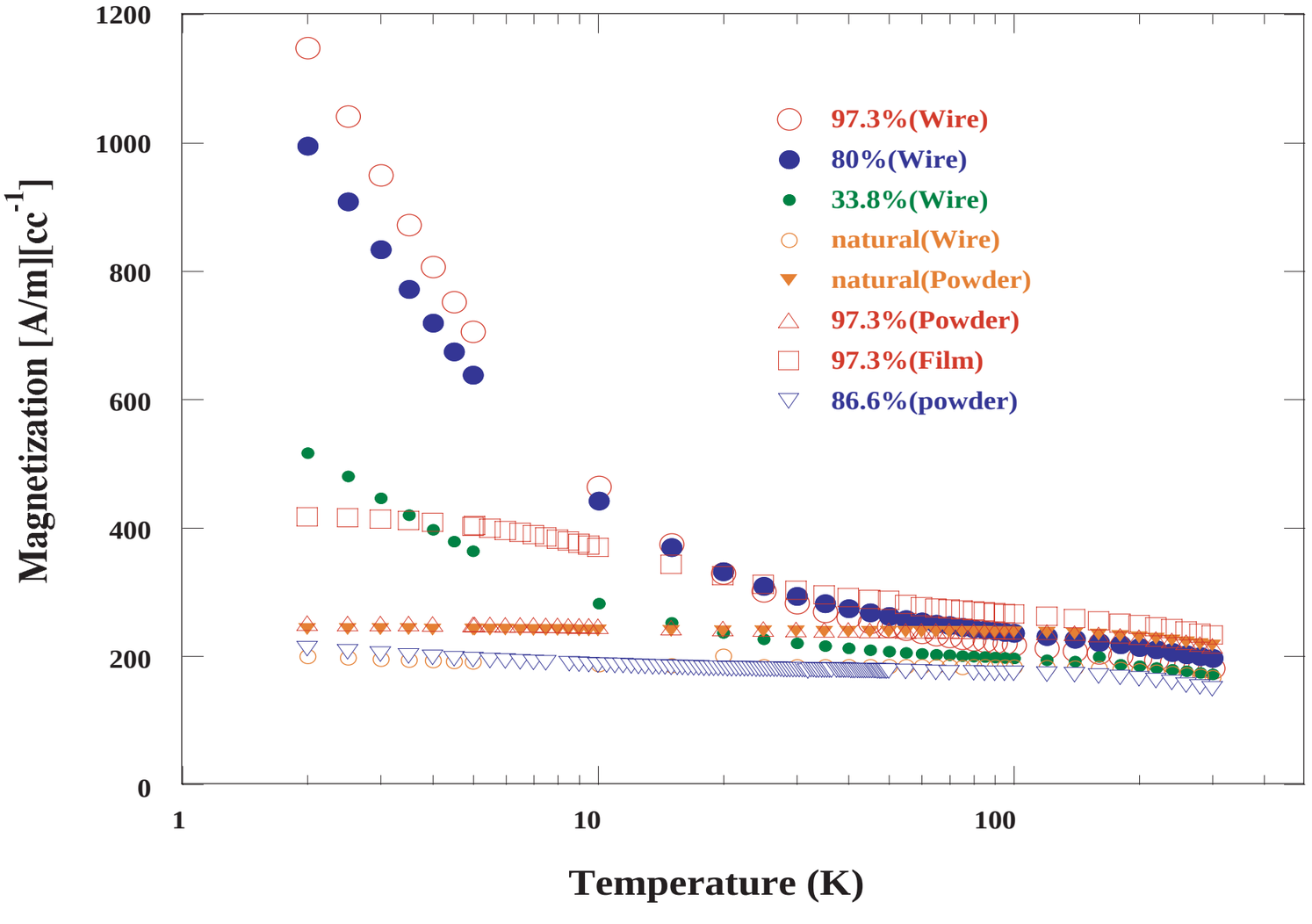
1200
1000
800
600
400
200
0
1
10
100
Magnetization [A/m][cc-1]
Temperature (K)
97.3%(Wire)
80%(Wire)
33.8%(Wire)
natural(Wire)
natural(Powder)
97.3%(Powder)
97.3%(Film)
86.6%(powder)

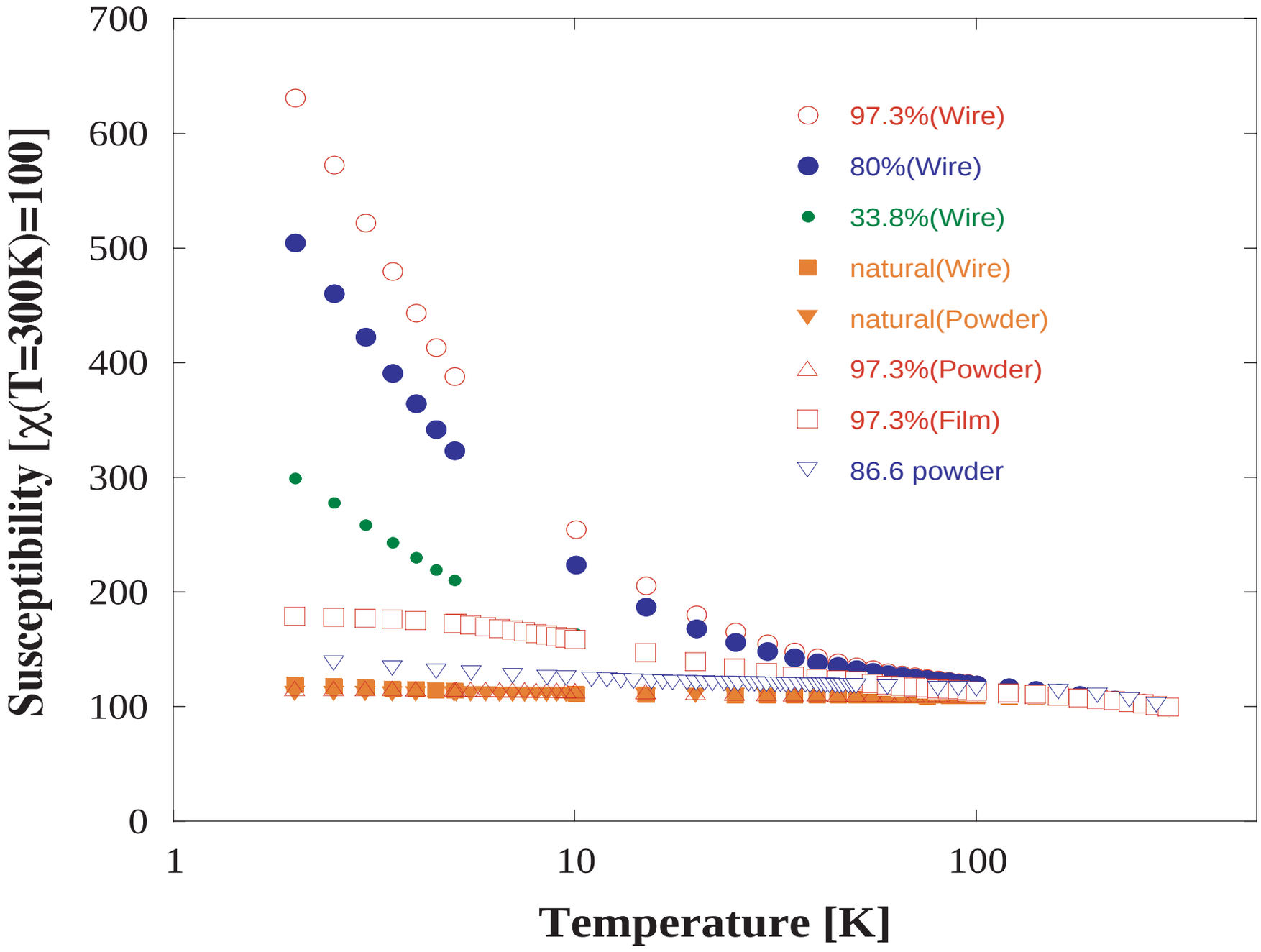
Susceptibility [χ(T=300K)=100]
700
600
500
400
300
200
100
0
1
10
100
Temperature [K]
97.3%(Wire)
80%(Wire)
33.8%(Wire)
natural(Wire)
natural(Powder)
97.3%(Powder)
97.3%(Film)
86.6 powder

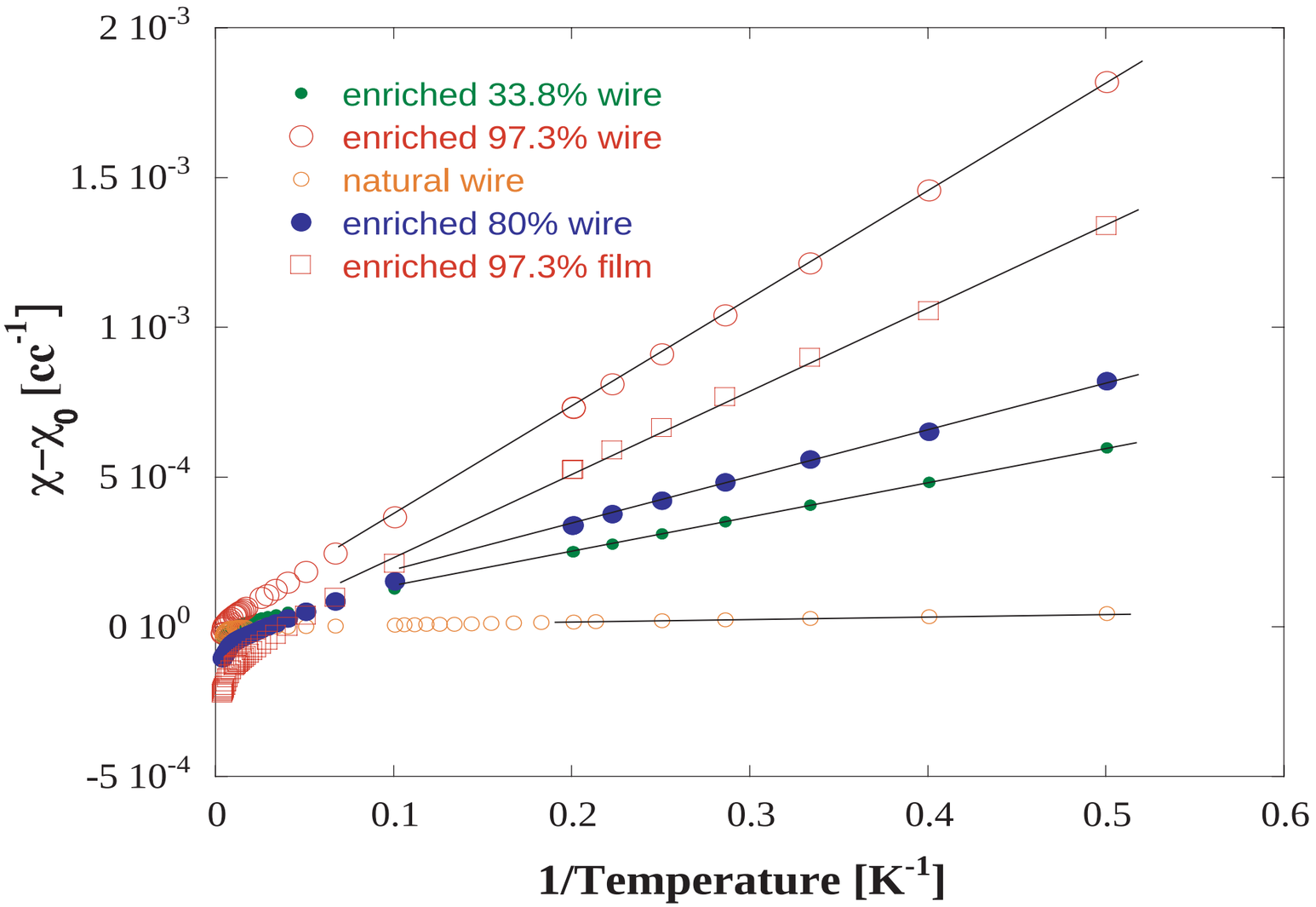
enriched 33.8% wire
enriched 97.3% wire
natural wire
enriched 80% wire
enriched 97.3% film
χ−χ0 [cc-1]
1/Temperature [K-1]
2 10-3
1.5 10-3
1 10-3
5 10-4
0 100
-5 10-4
0
0.1
0.2
0.3
0.4
0.5
0.6

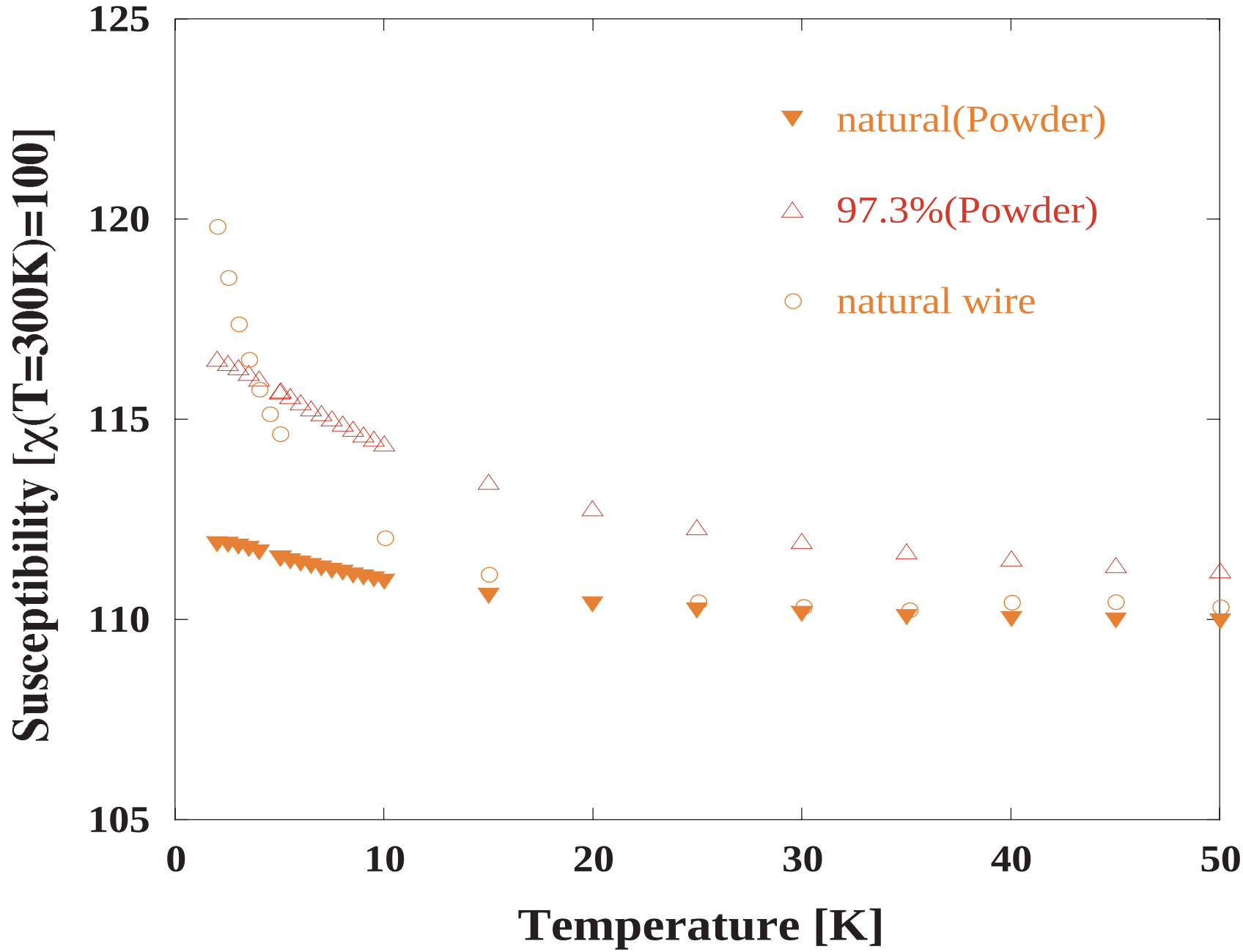
125
120
115
110
105
0
10
20
30
40
50
Susceptibility [χ(T=300K)=100]
Temperature [K]
natural(Powder)
97.3%(Powder)
natural wire

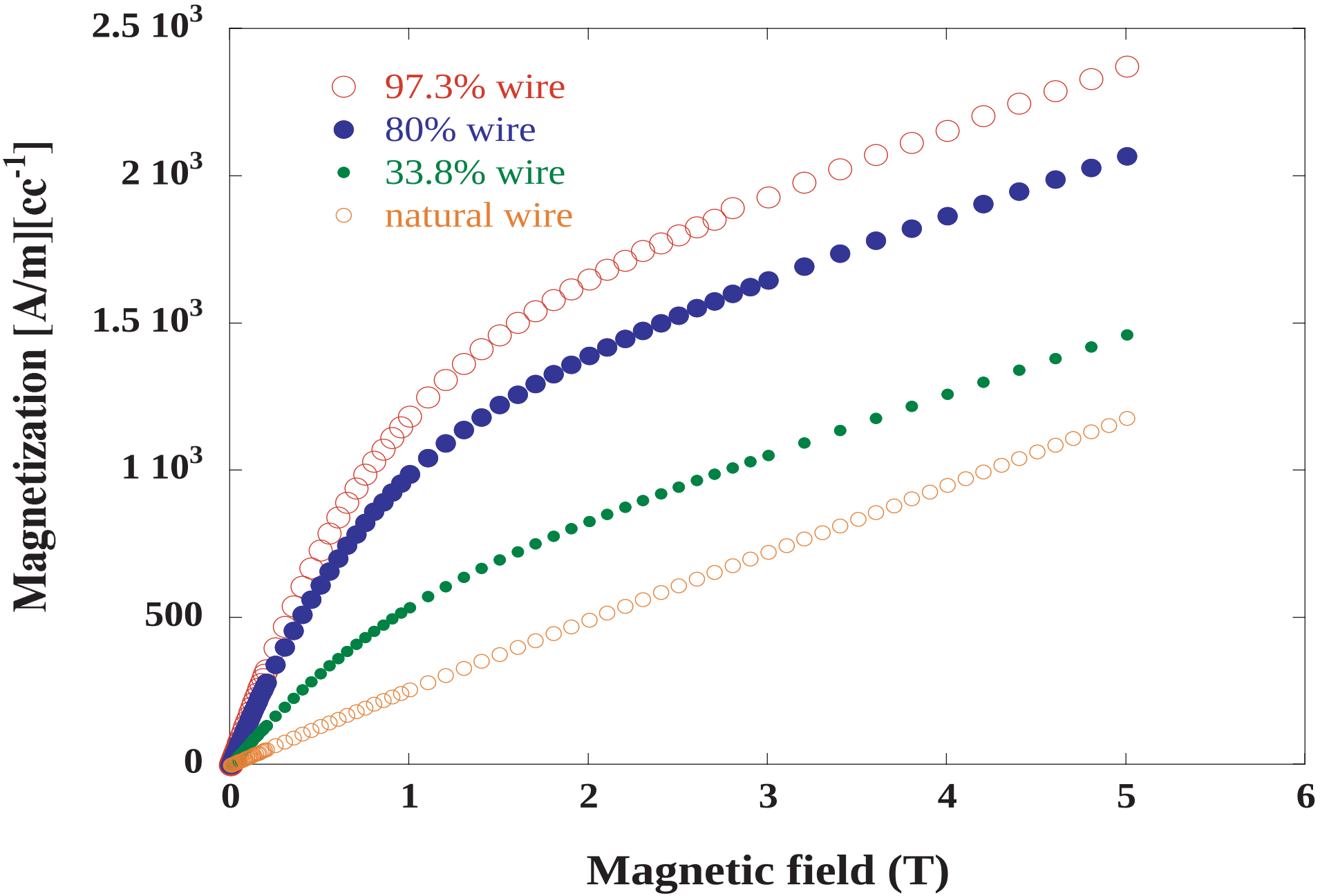
97.3% wire
80% wire
33.8% wire
natural wire
Magnetization [A/m][cc-1]
2.5 10^3
2 10^3
1.5 10^3
1 10^3
500
0
0
1
2
3
4
5
6
Magnetic field (T)

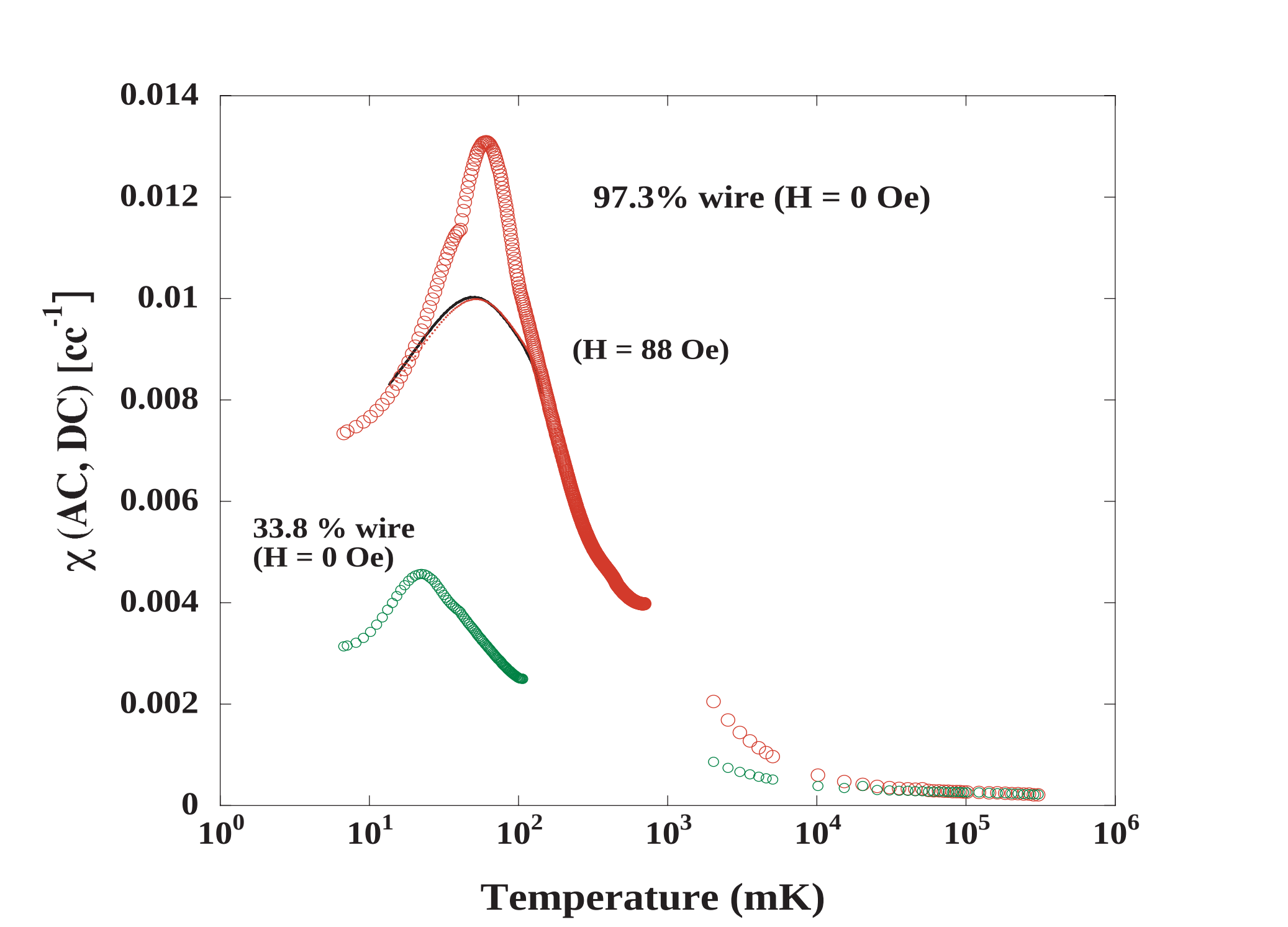
0.014
0.012
0.01
0.008
0.006
0.004
0.002
0
χ (AC, DC) [cc-1]
97.3% wire (H = 0 Oe)
(H = 88 Oe)
33.8 % wire
(H = 0 Oe)
10^0
10^1
10^2
10^3
10^4
10^5
10^6
Temperature (mK)

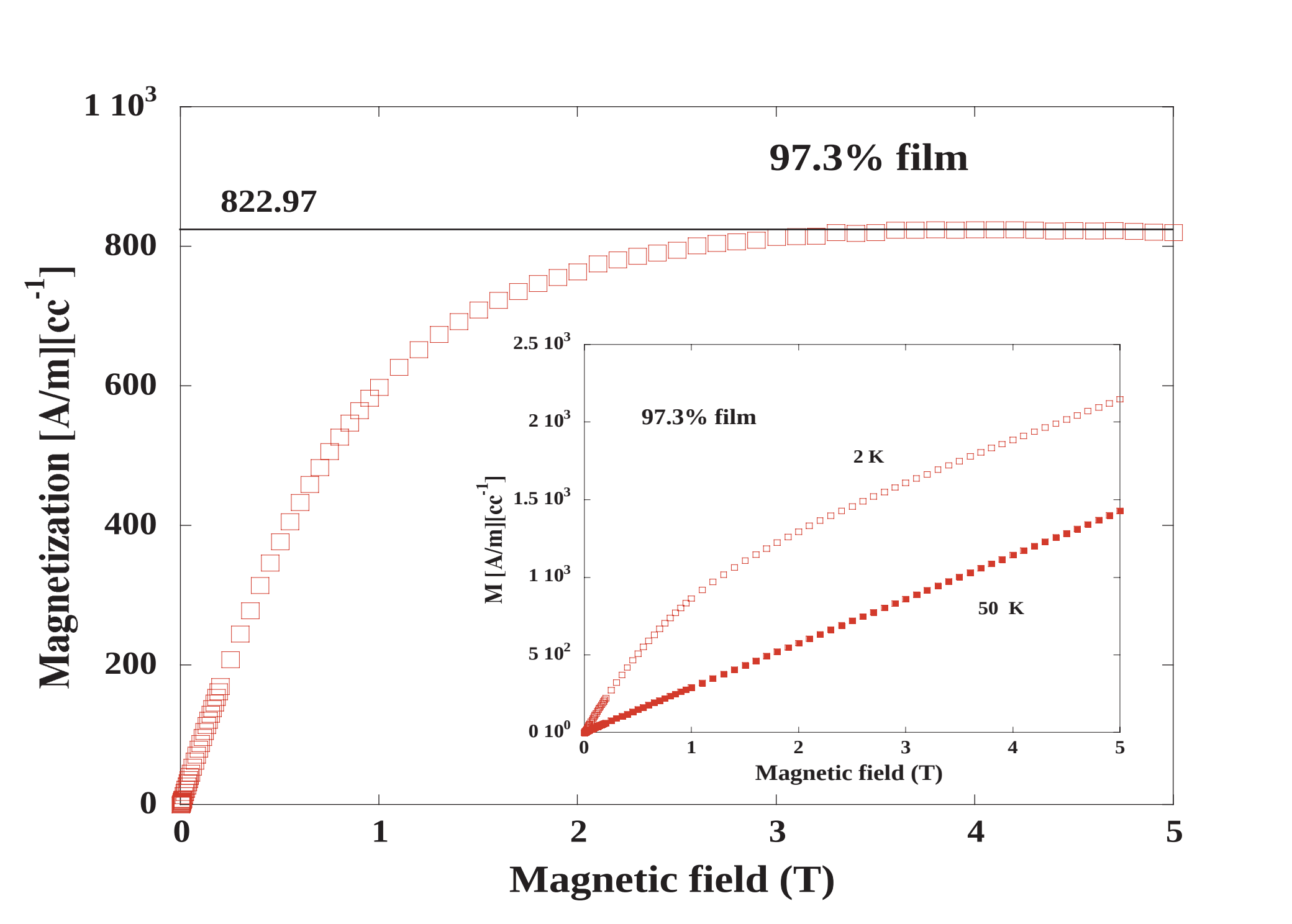
97.3% film
822.97
Magnetization [A/m][cc-1]
Magnetic field (T)
1 10^3
800
600
400
200
0
0
1
2
3
4
5
97.3% film
2 K
50 K
M [A/m][cc-1]
Magnetic field (T)
2.5 10^3
2 10^3
1.5 10^3
1 10^3
5 10^2
0 10^0

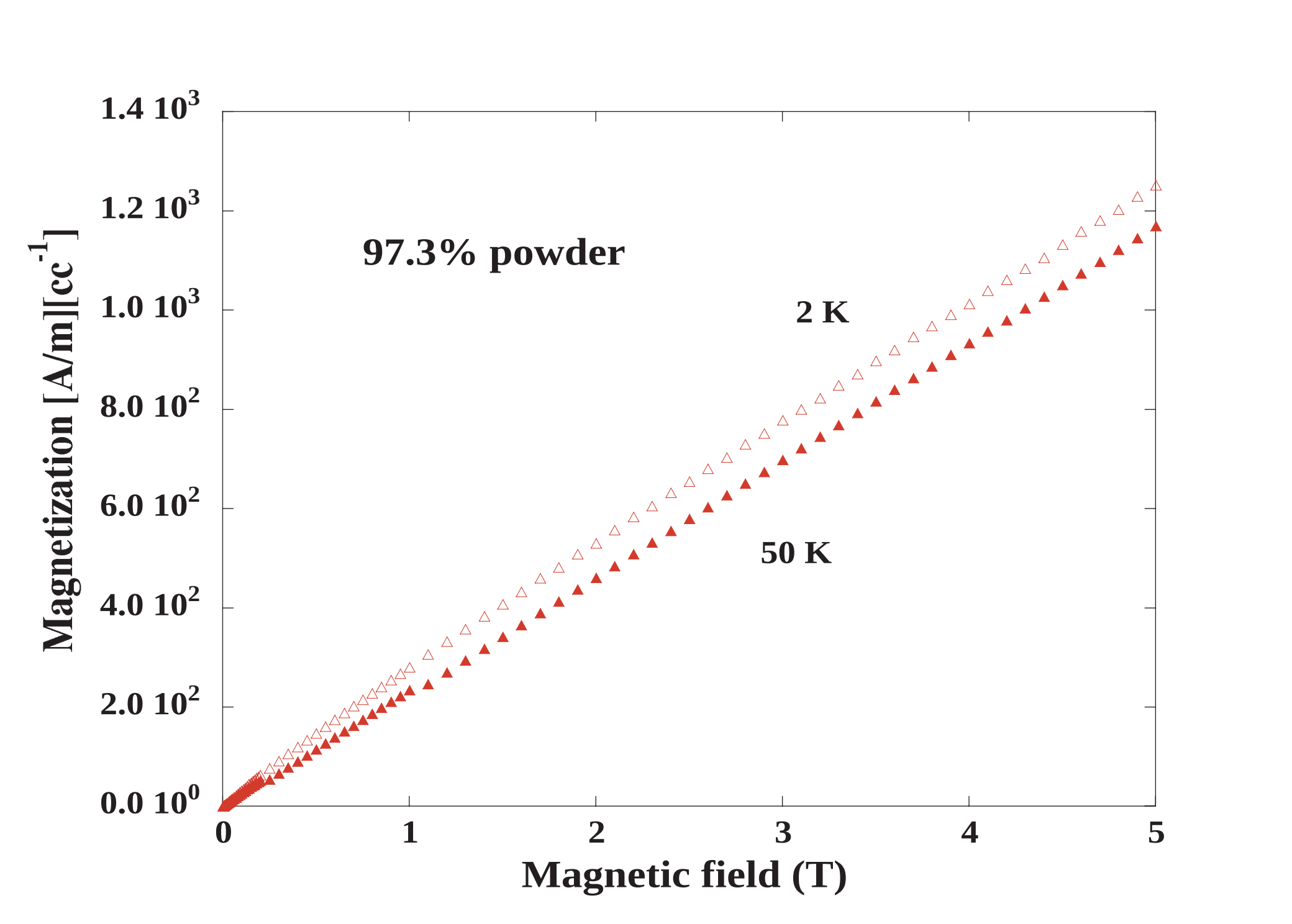
97.3% powder
2 K
50 K
Magnetization [A/m][cc^{-1}]
Magnetic field (T)
1.4 10^3
1.2 10^3
1.0 10^3
8.0 10^2
6.0 10^2
4.0 10^2
2.0 10^2
0.0 10^0
0
1
2
3
4
5

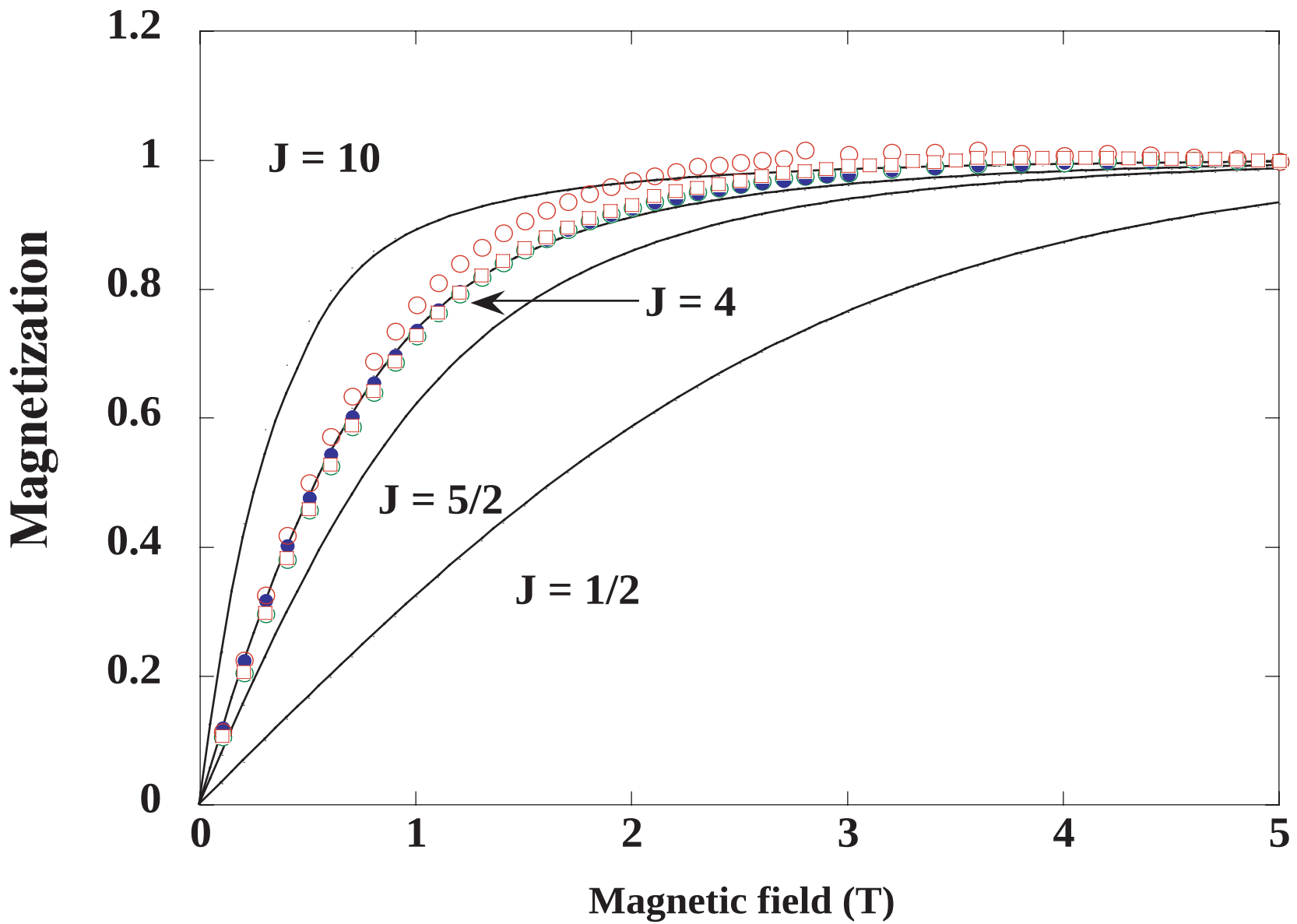
Magnetization
Magnetic field (T)
J = 10
J = 4
J = 5/2
J = 1/2
0
0.2
0.4
0.6
0.8
1
1.2
0
1
2
3
4
5

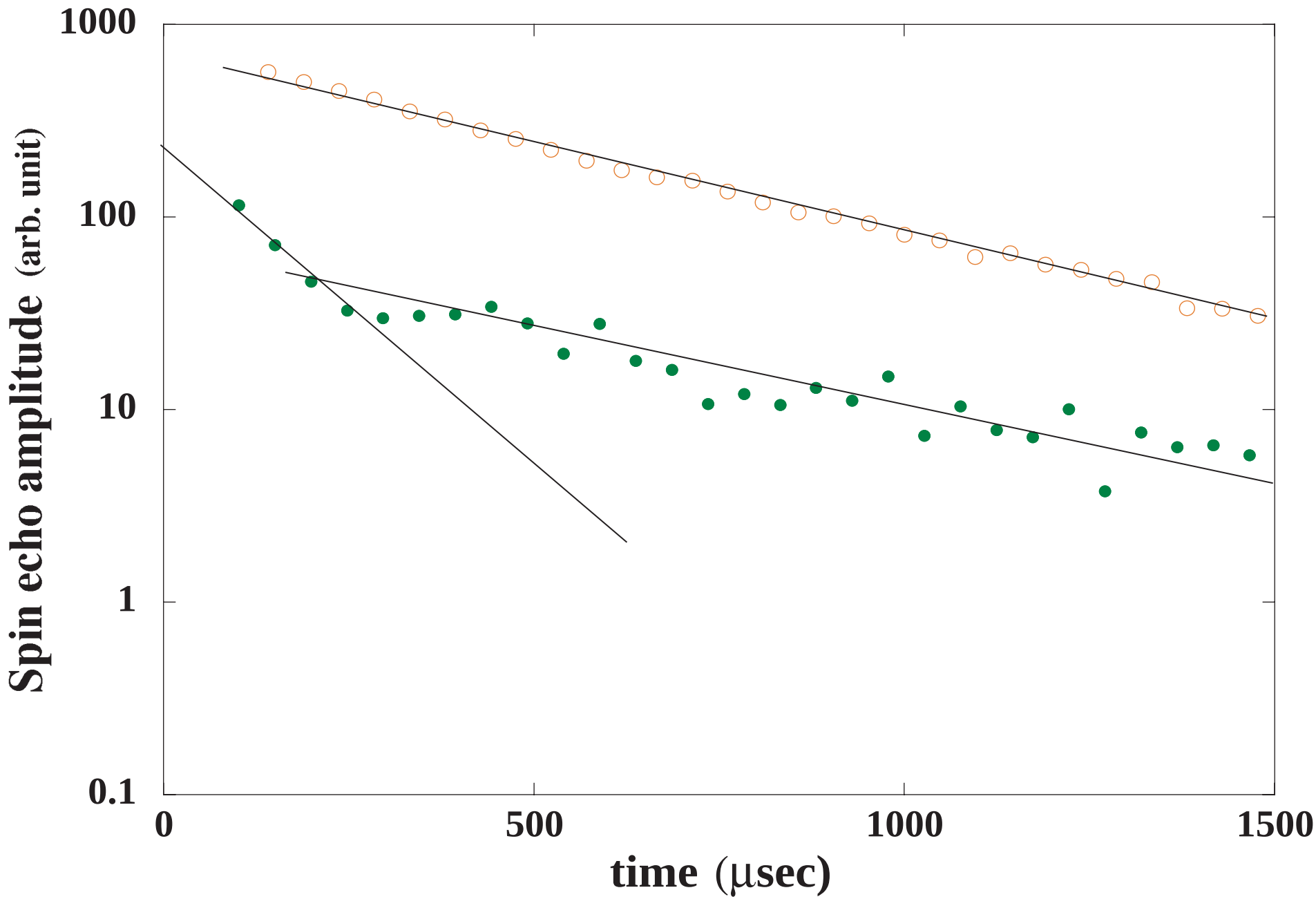
1000
100
10
1
0.1
Spin echo amplitude (arb. unit)
0
500
1000
1500
time (μsec)

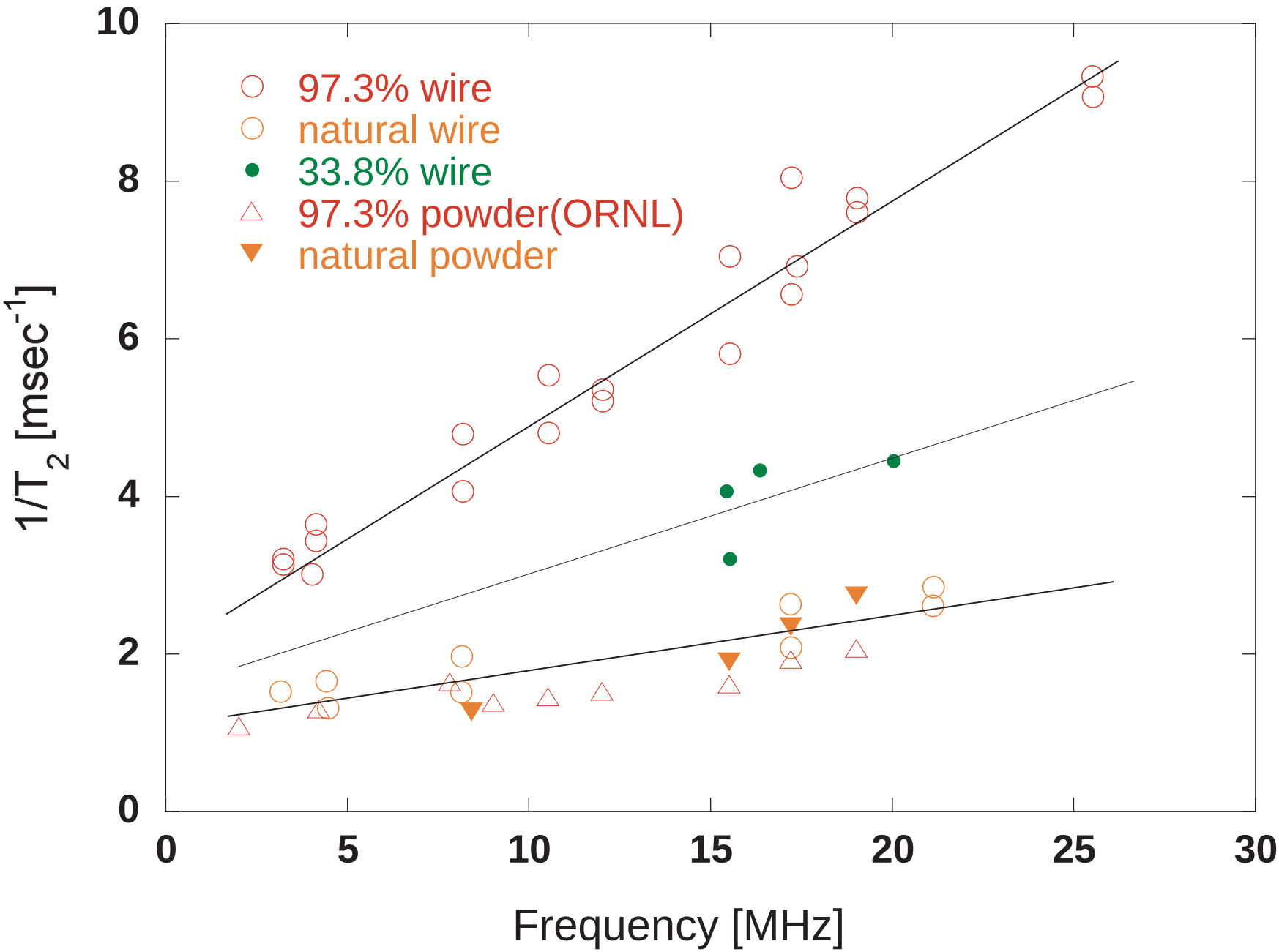
97.3% wire
natural wire
33.8% wire
97.3% powder(ORNL)
natural powder
1/T2 [msec-1]
Frequency [MHz]
0
2
4
6
8
10
0
5
10
15
20
25
30